AIAA JOURNAL
Vol. 44, No. 11, November 2006

# Flutter Analysis of Contra-Rotating Blade Rows

Masanobu Namba* and Ryohei Nishino†
*Sojo University, Kumamoto 860-0082, Japan*

DOI: 10.2514/1.22561

**To investigate the flutter characteristics of cascading blades in multiple blade rows, the computation program to calculate the unsteady blade loading based on the unsteady lifting surface theory for contra-rotating annular cascades was formulated and coded. Then a computation program to solve the coupled bending-torsion flutter equation for the contra-rotating annular cascades was also developed. Some results of the flutter analysis are presented. It is shown that the presence of the neighboring blade row gives rise to substantial change in the critical flutter condition irrespective of the blade row gap when the main acoustic duct mode is of cut-on state. The effect of the neighboring blade row is also significant irrespective of the state of the main acoustic duct mode when the blade rows are very closely placed.**

## Nomenclature

| | | |
|---|---|---|
| $\boldsymbol{A}$ | = | aerodynamic force matrix of flutter equation; Eqs. (15) and (21) |
| $a$ | = | displacement of a blade oscillation normal to blade surface; Eqs. (2) and (12) |
| $b$ | = | semichord of a blade |
| $b_a$ | = | axial semichord of a blade; Fig. 2 |
| $\boldsymbol{C}$ | = | coefficient matrix of flutter equation; Eqs. (23) and (25) |
| $C_a$ | = | axial chord length of a blade, or mean axial chord length of blades of rotor 1 and rotor 2 |
| $C_{aj}$ | = | axial chord length of blades of rotor $j$: $j = 1$ or 2 |
| $G$ | = | axial distance between the centers of rotor 1 and rotor 2; Fig. 1 |
| $h$ | = | hub-to-tip ratio |
| $\boldsymbol{I}$ | = | unit matrix |
| $\bar{I}_k$ | = | dimensionless generalized modal moment of inertia; Eqs. (20) and (B14) |
| $\boldsymbol{K}$ | = | stiffness matrix of flutter equation; Eqs. (15) and (20) |
| $k_\ell^{(n)}$ | = | radial eigenvalue of radial order $\ell$ and circumferential wave number $n$ |
| $L_{Bkj}$ | = | modal lift coefficient for bending motion; Eq. (B7) |
| $L_{Tkj}$ | = | modal lift coefficient for torsional motion; Eq. (B7) |
| $\ell$ | = | radial order of acoustic duct mode |
| $\boldsymbol{M}$ | = | mass matrix of flutter equation; Eqs. (15) and (18) |
| $M_a$ | = | axial flow Mach number |
| $\bar{M}_k$ | = | dimensionless generalized modal mass; Eqs. (18) and (B14) |
| $M_{Bkj}$ | = | modal moment coefficient for bending motion; Eq. (B8) |
| $M_{Tkj}$ | = | modal moment coefficient for torsional motion; Eq. (B8) |
| $N_{Bj}$ | = | number of blades of rotor $j$: $j = 1$ or 2 |
| $n_{\mu,\nu}$ | = | circumferential wave number of acoustic duct mode for harmonic parameters $\mu$ and $\nu$; Eq. (8) |
| $p_0^*$ | = | static pressure of undisturbed fluid |
| $\boldsymbol{q}$ | = | disturbance flow velocity; Eq. (A1) |
| $q_{\perp j}$ | = | disturbance flow velocity component normal to blade surface of rotor $j$: $j = 1$ or 2 |
| $r$ | = | radial coordinate; Fig. 1 |
| $r_e$ | = | dimensionless averaged radius of gyration of a blade; Eq. (B13) |
| $r_T^*$ | = | tip radius of the rotors, i.e., outer radius of the annular duct |
| $\boldsymbol{S}$ | = | static mass moment matrix of flutter equation; Eqs. (15) and (19) |
| $\bar{S}_{kj}$ | = | dimensionless generalized static mass moment; Eqs. (19) and (B14) |
| $s$ | = | local chordwise coordinate; Fig. 2 |
| $t$ | = | time coordinate |
| $W_a^*$ | = | axial flow velocity of undisturbed fluid |
| $W_{aF}$ | = | dimensionless flutter axial flow velocity; Eq. (34) |
| $W_{aF}^{(m)}$ | = | dimensionless flutter axial flow velocity of the $m$th flutter mode; Eq. (31) |
| $X$ | = | parameter defined by Eq. (24) |
| $x_{\mathrm{eg}}$ | = | dimensionless distance between the elastic axis and center of gravity of a blade; Eq. (B13) |
| $Z_j(r)$ | = | modal shape function of $j$th bending mode |
| $z$ | = | axial coordinate |
| $z_j$ | = | axial coordinate for coordinate system fixed to rotor $j$: $j = 1$ or 2 |
| $\Delta p_{j,(\nu)}$ | = | $\nu$th harmonic component of unsteady pressure difference across a blade of rotor $j$ |
| $\delta_{kj}$ | = | Kronecker delta |
| $\eta(r,t)$ | = | bending displacement normal to a blade surface; Fig. 2 |
| $\eta_j$ | = | modal amplitude of $j$th mode bending oscillation; Eq. (13) |
| $\theta$ | = | angular coordinate in the cylindrical coordinate system fixed to the duct |
| $\theta_j$ | = | angular coordinate in the cylindrical coordinate system fixed to rotor $j$ |
| $\lambda$ | = | reduced frequency; Eq. (16) |
| $\lambda_{Bj}$ | = | reduced natural frequency of $j$th mode bending oscillation; Eq. (22) |
| $\lambda_F^{(m)}$ | = | reduced flutter frequency of $m$th flutter mode; Eq. (30) |
| $\lambda_{Tj}$ | = | reduced natural frequency of $j$th mode torsional oscillation; Eq. (22) |
| $\mu$ | = | harmonic number |
| $\mu_{ba}$ | = | mass ratio of a blade; Eq. (B13) |
| $\nu$ | = | harmonic number |
| $\xi_j$ | = | helical coordinate in the frame of reference fixed to rotor $j$; Eq. (A2) |
| $\rho_0^*$ | = | density of undisturbed fluid |
| $\sigma$ | = | interblade phase parameter: of blade oscillation; Eq. (2) |
| $\sigma_{j\nu}$ | = | interblade phase parameter of unsteady blade loading of harmonic number $\nu$ of rotor $j$; Eqs. (3–6) |

Presented as Paper 19 at the 43rd AIAA Aerospace Science Meeting and Exhibit, Reno, NV, 10–12 January 2005; received 19 January 2006; revision received 7 April 2006; accepted for publication 8 May 2006. 

*Professor, Department of Aerospace Systems Engineering; namba@arsp.sojo-u.ac.jp. Senior Member AIAA.

†Graduate Student, Department of Aerospace Systems Engineering

$\Phi_j(r)$ = modal shape function of $j$th torsional mode
$\phi(r,t)$ = angular displacement of blade oscillation; Fig. 2
$\phi_j$ = modal amplitude of $j$th torsional mode oscillation; Eq. (13)
$\Omega_j$ = dimensionless angular velocity of rotor $j$, $\Omega_j^* r_T^*/W_a^*$
$\omega$ = reduced angular frequency of blade oscillation, $\omega^* r_T^*/W_a^*$
$\omega_{j\nu}$ = reduced frequency of unsteady blade loading of harmonic number $\nu$ of rotor $j$; Eqs. (3–6)
$\omega_{\mu,\nu}$ = reduced frequency of acoustic duct mode of harmonic parameters $\mu$ and $\nu$; Eq. (7)
$\omega_F^{(m)}$ = dimensionless flutter frequency of $m$th flutter mode; Eq. (31)
$\omega^{\pm}_{\mu,\nu,\ell}$ = cutoff reduced frequency of acoustic duct mode $(\mu,\nu;\ell)$; Eq. (11)
$\bar{\omega}_{Bk}$ = dimensionless natural frequency of $k$th bending mode; Eq. (26)
$\bar{\omega}_{Tk}$ = dimensionless natural frequency of $k$-th torsional mode; Eq. (26)

## I. Introduction

THE axial turbomachines are in general composed of multiple blade rows, which are closely placed. On the other hand it is well known that the unsteady aerodynamic force on oscillating blades in a cascade is heavily dependent on the interblade phase angle. This implies that the aerodynamic coupling among blades plays a critical role on the cascade flutter characteristics. From this standpoint it is quite reasonable to expect that neighboring blade rows, e.g., a neighboring rotor or stator or contra-rotating fan cascade, also will have a considerable influence on the unsteady aerodynamic force on vibrating blades and the cascade flutter conditions.

The authors would like to point out that the pioneering studies on the problem of the influence of neighboring blade rows on the unsteady aerodynamic response of oscillating blades were conducted by Japanese researchers in the 1960s and 1970s. The theoretical study based on the semiactuator disk model by Tanida [1] and the experiments and the linear cascade theory by Kobayashi et al. [2,3] should be cited as the earliest works. Their works show only a minor importance of the multistage coupling for the cascade flutter. This is one of the reasons that the problem was left unstudied further. We should note, however, that their theories assume incompressible flows and therefore can not deal with aeroacoustic interaction between blade rows via cut-on acoustic duct modes.

Since then until recently no paper dealing with the subject was published except a Russian paper by Butenko and Osipov [4], which developed a theory for subsonic linear cascades in relative motion.

The extension of the study of the cascade flutter to multistage cascades is recently drawing a renewed interest of turbomachinery aerodynamicists. Hall and Silkowski [5] presented an analysis based on two-dimensional subsonic multiple blade rows, and Namba et al. [6] developed a three-dimensional lifting surface theory for oscillating subsonic contra-rotating annular cascades. Those studies for subsonic flows indicate that the influence of aeroacoustic coupling among blade rows on the aerodynamic damping force is significant in particular when the main acoustic duct mode generated from the oscillating blade row is cut-on.

Namba and Nanba [7] extended the three-dimensional lifting surface theory so that it can deal with the combination of supersonic and subsonic cascades, for instance, a supersonic rotor cascade and a subsonic stator cascade, and further applied it to flutter analysis. Hall et al. [8] developed a three-dimensional Euler solver for computing unsteady flows in vibrating multistage cascades. It should be noted, in particular, that in their paper comparison is made of a model problem between the computations by their Euler solver and the author's lifting surface theory, and an excellent agreement is demonstrated.

This paper presents further details of the method of flutter analysis. The present computation program based on the unsteady lifting surface theory is formulated so that it can provide aerodynamic forces on oscillating blades as functions of the frequency. As a natural advantage of the analytical method over CFD, the computation speed is remarkably high, so that it can be a very efficient tool to calculate aerodynamic force terms of the flutter equations.

A computation program to solve the coupled bending-torsion flutter equation for the contra-rotating annular cascades was also formulated and coded. This paper provides some numerical results of flutter analysis and investigates how the cascade flutter conditions are influenced by presence of the neighboring blade row in relative rotational motion.

## II. Outline of the Analytical Method

### A. Model Description

We consider a pair of annular cascades in an annular duct of infinite axial extent with the outer duct radius $r_T^*$ and the boss ratio $h$ as shown in Fig. 1. The undisturbed flow is a uniform axial flow of axial velocity $W_a^*$, static pressure $p_0^*$, and fluid density $\rho_0^*$. In the following, unstarred symbols denote dimensionless quantities, where lengths, velocities, pressures, and times are scaled with respect to $r_T^*$, $W_a^*$, $\rho_0^* W_a^{*2}$, and $r_T^*/W_a^*$, respectively. Let subscripts 1 and 2 denote the upstream rotor 1 and the downstream rotor 2, respectively. Further following notations are used: $\Omega_1 = \Omega_1^* r_T^*/W_a^*$ ($\geq 0$, clockwise looking from a downstream station) and $\Omega_2 = \Omega_2^* r_T^*/W_a^*$ ($\leq 0$ anticlockwise): rotational angular velocities of the rotors; $C_{a1}$ and $C_{a2}$: axial chord lengths of blades assumed constant along the span; and $(r,\theta,z)$, $(r,\theta_1,z_1)$, and $(r,\theta_2,z_2)$: cylindrical coordinates in the frames fixed to the duct, rotor 1, and rotor 2, respectively. The angle coordinates and axial coordinates of different frames are related to each other by

$$\theta = \theta_1 - \Omega_1 t = \theta_2 - \Omega_2 t, \qquad z = z_1 = z_2 + G \tag{1}$$

We assume that the steady blade loading is zero, i.e., the time mean flow is uniform, and that the unsteady disturbances induced by blade vibrations are small. Therefore the unsteady flow is governed by linearized equations.

### B. Multiplication of Blade Loading Frequency

Assume that all blades of rotor 1 are vibrating with a single frequency $\omega(=\omega^* r_T^*/W_a^*)$ and an interblade phase angle $2\pi\sigma/N_{B1}$, so that the displacement normal to the blade surface of the $m$th blade is given by

$$a(r,z)e^{i\omega t + i2\pi\sigma m/N_{B1}}:\ m = 0, 1, \cdots, N_{B1}-1 \tag{2}$$

Here $\sigma$ is an integer between $-N_{B1}/2$and $N_{B1}/2$.

Then as described in detail in [6], aeroacoustic coupling between the rotors in mutual motion produces flow disturbances of multiple frequencies, resulting in blade loading of multiple frequencies. Thus we can describe the unsteady blade loading (pressure difference between upper and lower surfaces of blades) on the $m$th blade of rotor 1 and rotor 2 as summations of multiple frequency components:

$$\sum_{\nu=-\infty}^{\infty} \Delta p_{1,(\nu)}(r,z_1)e^{i\omega_{1\nu}t + i2\pi\sigma_{1\nu}m/N_{B1}} \tag{3}$$

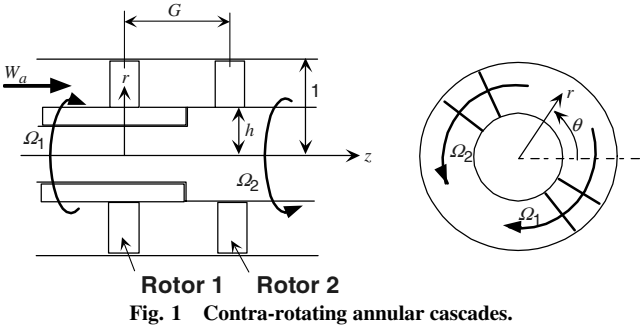


**Fig. 1 Contra-rotating annular cascades.**

and

$$\sum_{\mu=-\infty}^{\infty} \Delta p_{2,(\mu)}(r, z_1) e^{i\omega_{2\mu} t + i2\pi\sigma_{2\mu} m/N_{B2}} \tag{4}$$

where

$$\omega_{1\nu} = \omega - \nu N_{B2}(\Omega_1 - \Omega_2), \qquad \sigma_{1\nu} = \nu N_{B2} + \sigma \tag{5}$$

$$\omega_{2\mu} = \omega - (\mu N_{B1} + \sigma)(\Omega_2 - \Omega_1), \qquad \sigma_{2\mu} = \mu N_{B1} + \sigma \tag{6}$$

It is worth emphasizing that all frequency components are coupled with each other and cannot be determined independently.

In the case of blade vibration of rotor 2, similar formulations can be made, but they are omitted to save space.

### C. Acoustic Modes and Frequencies

In the present problem disturbances are composed of multiple frequencies and multiple acoustic duct modes. In the case of blade vibration of rotor 1, the frequencies $\omega_{\mu,\nu}$ viewed in the frame of reference fixed to the duct, i.e., $(r, \theta, z)$ system, and corresponding circumferential wave numbers $n_{\mu,\nu}$ of the duct modes are given by

$$\omega_{\mu,\nu} = \omega + (\mu N_{B1} + \sigma)\Omega_1 + \nu N_{B2}\Omega_2 \tag{7}$$

and

$$n_{\mu,\nu} = \mu N_{B1} + \nu N_{B2} + \sigma \tag{8}$$

Hereafter we denote the acoustic duct mode of $(n_{\mu,\nu}, \ell)$ by $(\mu, \nu; \ell)$. A mode $(\mu, \nu; \ell)$ is cut off if

$$\left(k_\ell^{(n_{\mu,\nu})}\right)^2 - \omega_{\mu,\nu}^2 M_a^2 / \left(1 - M_a^2\right) > 0 \tag{9}$$

where $k_\ell^{(n)}$ denotes the radial eigenvalue [9,10]. Solving the inequality (9) for the blade vibration frequency $\omega$, we can write

$$\omega_{\mu,\nu,\ell}^-(\sigma) < \omega < \omega_{\mu,\nu,\ell}^+(\sigma) \tag{10}$$

where the critical cutoff frequencies are given by

$$\omega_{\mu,\nu,\ell}^{\pm}(\sigma) = \pm k_\ell^{(n_{\mu,\nu})} \sqrt{1 - M_a^2}/M_a - (\mu N_{B1}\Omega_1 + \nu N_{B2}\Omega_2 + \sigma\Omega_1) \tag{11}$$

in the case of vibration of rotor 1 blades. Note that the expression for the case of vibration of rotor 2 blades can simply be obtained by exchanging the subscript 1 for 2 and 2 for 1.

Under this notation of the duct modes we can state that vibrating blades directly generate $(\mu, 0; \ell)$ modes. Hereafter let us call the modes of $\nu = 0$ the primary duct modes, and the modes of $\nu \neq 0$ the secondary duct modes.

If all of the primary duct modes are cut off and if the rotors are remotely separated, the influence of the neighboring blade row will not be substantial. We should note, however, that there exist vortical disturbances that are convected without decaying under the assumption of inviscid flows. Therefore, in the case of vibration of rotor 1, the vortical disturbances from rotor 1 always exert a finite influence on rotor 2 even if all primary duct modes $(\mu, 0; \ell)$ are cut off, and however large the rotor-to-rotor distance $G$ may be. Further, any of the secondary duct modes of $\nu \neq 0$ resulting from the interaction can be cut on, giving backward reaction to rotor 1. The previous studies [6] indicate, however, that the vortical disturbances play only a minor role in the aerodynamic interaction between the blade rows.

Note that $\Omega_1\Omega_2 < 0$ in the case of contra-rotating cascades. Therefore duct modes of $\mu\nu > 0$ are of high frequency and low circumferential wave number, and are likely to satisfy the cut-on condition.

### D. Determination of Aerodynamic Force

The lifting surface theory expresses the disturbance flowfield as summation of disturbances induced by unsteady blade loadings of both rotors. The disturbance flow quantities are mathematically expressed in integral forms, the integrands of which involve a blade loading function multiplied by a kernel function. Once the blade loading functions are determined, the disturbance flow quantities are obtained by straightforward computation of the integrals.

In the present problem the blade loading functions are not prescribed but are unknown functions to be determined. The flow tangency condition at the blade surfaces gives a set of simultaneous integral equations for the unsteady blade loading functions $\Delta p_{1,(\nu)}(r, z_1)$: $\nu = 0, \pm1, \pm2, \cdots$ and $\Delta p_{2,(\mu)}(r, z_2)$: $\mu = 0, \pm1, \pm2, \cdots$, as shown in Appendix A. There are available various methods to solve the equations numerically. A method based on combination of Galerkin formulation and expansion of blade loading functions in terms of double mode function series is applied to the present study. Details are omitted to save space.

### E. Coupled Bending-Torsion Vibration of Blades

Consider the blades of either of the rotors are oscillating at a frequency $\omega$ and an interblade phase angle $2\pi\sigma/N_B$. Hereafter the suffix 1 or 2 denoting the rotor number is omitted. As shown in Fig. 2 we describe the displacement of a blade normal to the blade surface by

$$a(r, s, t) = \eta(r, t) + \{s - s_e(r)\}\phi(r, t) \tag{12}$$

where $\phi(r, t)$ denotes the torsional displacement about an elastic axis $s = s_e(r)$. Here $s$ denotes a local chordwise coordinate, i.e., $\mathrm{d}s = \sqrt{1 + \Omega^2 r^2}\,\mathrm{d}z$. Further express the bending and torsional displacements by

$$\eta(r, t) = e^{i\omega t} \sum_{j=1}^{\infty} Z_j(r)\eta_j, \qquad \phi(r, t) = e^{i\omega t} \sum_{j=1}^{\infty} \Phi_j(r)\phi_j \tag{13}$$

where $Z_j(r)$ and $\Phi_j(r)$ denote normalized bending and torsional natural mode shape functions of order $j$ respectively, and $\eta_j$ and $\phi_j$ denote the modal amplitudes, which are complex numbers. The natural modes imply the free vibration modes in vacuum.

As described by Eq. (3), the aerodynamic force on vibrating blades under the aerodynamic interaction between the two blade rows is of multiple frequencies, but one should note that the blade motion of the frequency $\omega$ can only be excited or damped by the fundamental frequency component $\nu = 0$ of the aerodynamic force.

Therefore let the fundamental frequency component of the blade surface pressure difference due to the blade motion described by Eqs. (12) and (13) be expressed by

$$\Delta p(r, s, t) = \sum_{j=1}^{\infty} \Delta p_{Bj}(r, s)\eta_j e^{i\omega t}/b_a + \sum_{j=1}^{\infty} \Delta p_{Tj}(r, s)\phi_j e^{i\omega t} \tag{14}$$

Here $\Delta p_{Bj}(r, s)\eta_j e^{i\omega t}/b_a$ and $\Delta p_{Tj}(r, s)\phi_j e^{i\omega t}$ denote the unsteady lifting pressure due to $j$th mode bending motion $[Z_j(r)\eta_j e^{i\omega t}]$ and the

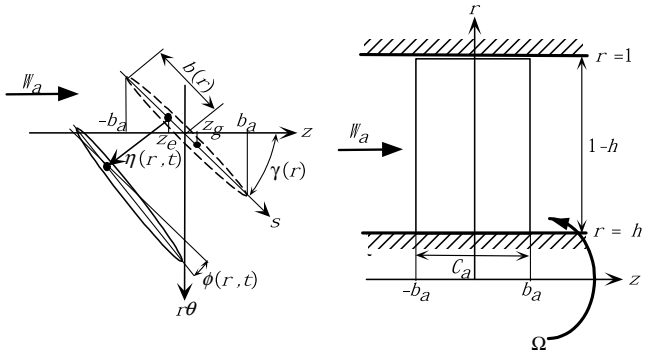


**Fig. 2 An oscillating blade in a rotating annular cascade.**

unsteady lifting pressure due to $j$th mode torsional motion $[\Phi_j(r)\phi_j e^{i\omega t}]$ about $s = s_e(r)$, respectively. Here $b_a = C_a/2$ denotes the semiaxial-chord.

Note again that blades are aerodynamically coupled although they are mechanically decoupled. Therefore the lifting pressure includes the effect of the aerodynamic coupling among all blades of both blade rows.

Neglecting the mechanical damping, we can describe the equation of the blade motion as a balance of the inertia, stiffness, and aerodynamic forces as follows:

$$-\lambda^2(\boldsymbol{M}+\boldsymbol{S})\boldsymbol{y}+\boldsymbol{K}\boldsymbol{y}=\boldsymbol{A}\boldsymbol{y} \tag{15}$$

where the reduced frequency is defined by

$$\lambda = \omega b_a = \omega^* b_a^*/W_a^* \tag{16}$$

and $\boldsymbol{y}$ denotes the blade displacement, which is a column vector:

$$\boldsymbol{y}=\begin{Bmatrix}\boldsymbol{y}_1\\ \boldsymbol{y}_2\\ \vdots\end{Bmatrix}, \qquad \boldsymbol{y}_k=\begin{Bmatrix}\eta_k/b_a\\ \phi_k\end{Bmatrix} \tag{17}$$

On the other hand, $\boldsymbol{M}$, $\boldsymbol{S}$, $\boldsymbol{K}$, and $\boldsymbol{A}$ are, respectively, mass, static mass moment, stiffness, and aerodynamic force matrices, the $kj$th elements of which are given by the following $2\times 2$ submatrices:

$$\boldsymbol{M}_{kj}=\mu_{\mathrm{ba}}\begin{bmatrix}\bar{M}_k & 0\\ 0 & r_e^2\bar{I}_k\end{bmatrix}\delta_{kj} \tag{18}$$

$$\boldsymbol{S}_{kj}=\mu_{\mathrm{ba}}x_{\mathrm{eg}}\begin{bmatrix}0 & \bar{S}_{kj}\\ \bar{S}_{jk} & 0\end{bmatrix} \tag{19}$$

$$\boldsymbol{K}_{kj}=\mu_{\mathrm{ba}}\begin{bmatrix}\bar{M}_k\lambda_{Bk}^2 & 0\\ 0 & r_e^2\bar{I}_k\lambda_{Tk}^2\end{bmatrix}\delta_{kj} \tag{20}$$

$$\boldsymbol{A}_{kj}=\begin{bmatrix}L_{Bkj} & L_{Tkj}\\ M_{Bkj} & M_{Tkj}\end{bmatrix} \tag{21}$$

Further,

$$\lambda_{Bk}=\omega_{Bk}^* b_a^*/W_a^*, \qquad \lambda_{Tk}=\omega_{Tk}^* b_a^*/W_a^* \tag{22}$$

denote dimensionless bending and torsional natural mode frequencies of order $k$. The definitions of the mass ratio $\mu_{ba}$, the averaged dimensionless radius of gyration $r_e$, the averaged dimensionless distance between the center of gravity and the elastic axis $x_{\mathrm{eg}}$, the dimensionless generalized modal mass $\bar{M}_k$, modal moment of inertia $\bar{I}_k$, and modal static mass moment $\bar{S}_{kj}$, and the dimensionless generalized modal aerodynamic forces $L_{Bkj}$, $L_{Tkj}$, $M_{Bkj}$, and $M_{Tkj}$ are given in Appendix B. At this stage it will be worth adding that the effect of the presence of the neighboring blade row is produced solely through the aerodynamic force terms in the flutter equation.

### F. Determination of Flutter Condition

After some algebraic manipulations Eq. (15) can be rewritten into

$$|\boldsymbol{C}-X\boldsymbol{I}|\boldsymbol{y}=0 \tag{23}$$

Here $X$ is defined by

$$X=\lambda_{B1}^2/\lambda^2=\omega_{B1}^{*2}/\omega^{*2} \tag{24}$$

Further, $\boldsymbol{C}$ is a complex matrix, $kj$th element of which is given by a submatrix:

$$\boldsymbol{C}_{kj}=\begin{bmatrix}\delta_{kj}/\bar{\omega}_{Bk}^2 & x_{\mathrm{eg}}\bar{S}_{kj}/\left(\bar{\omega}_{Bk}^2\bar{M}_k\right)\\ x_{\mathrm{eg}}\bar{S}_{jk}/\left(\bar{\omega}_{Tk}^2 r_e^2\bar{I}_k\right) & \delta_{kj}/\bar{\omega}_{Tk}^2\end{bmatrix} + \frac{1}{\mu_{ba}\lambda^2}\begin{bmatrix}L_{Bkj}/\left(\bar{\omega}_{Bk}^2\bar{M}_k\right) & L_{Tkj}/\left(\bar{\omega}_{Bk}^2\bar{M}_k\right)\\ M_{Bkj}/\left(\bar{\omega}_{Tk}^2 r_e^2\bar{I}_k\right) & M_{Tkj}/\left(\bar{\omega}_{Tk}^2 r_e^2\bar{I}_k\right)\end{bmatrix} \tag{25}$$

where

$$\bar{\omega}_{Bk}=\lambda_{Bk}/\lambda_{B1}=\omega_{Bk}^*/\omega_{B1}^*, \qquad \bar{\omega}_{Tk}=\lambda_{Tk}/\lambda_{B1}=\omega_{Tk}^*/\omega_{B1}^* \tag{26}$$

Then $X$ and $\boldsymbol{y}$ can be determined as eigenvalues and eigenvectors of the matrix $\boldsymbol{C}$, respectively. Let the eigenvalues and eigenvectors be denoted by

$$\boldsymbol{X}=\begin{bmatrix}X^{(1)} & X^{(2)} & \cdots\end{bmatrix} \quad \text{and} \quad \boldsymbol{Y}=\begin{bmatrix}\boldsymbol{y}^{(1)} & \boldsymbol{y}^{(2)} & \cdots\end{bmatrix}=\begin{bmatrix}\boldsymbol{y}_1^{(1)} & \boldsymbol{y}_1^{(2)} & \cdots\\ \boldsymbol{y}_2^{(1)} & \boldsymbol{y}_2^{(2)} & \cdots\\ \vdots & \vdots & \ddots\end{bmatrix} \tag{27}$$

respectively, where

$$\boldsymbol{y}_k^{(m)}=\begin{Bmatrix}\eta_k^{(m)}/b_a\\ \phi_k^{(m)}\end{Bmatrix} \tag{28}$$

Now note that the matrix $\boldsymbol{C}$ is governed by elastic and structural parameters: $\mu_{\mathrm{ba}}$, $x_{\mathrm{eg}}$, $r_e$, $\bar{M}_k$, $\bar{I}_k$, $\bar{S}_{kj}$, $\bar{\omega}_{Bk}$, and $\bar{\omega}_{Tk}$, and parameters of blade row configuration on which the aerodynamic force terms are dependent: $\Omega_1$, $\Omega_2$ (rotational speeds), $N_{B1}$, $N_{B2}$, $C_{a1}$, $C_{a2}$, $h$ (boss ratio), $G$, $M_a$, $\lambda$, $\sigma$, and the blade profile shapes.

Let all elastic and aerodynamic parameters other than $\lambda$ be specified. Then the eigenvalues $X^{(m)}$: $m=1,2,\cdots$ and the eigenvectors $\boldsymbol{y}^{(m)}$: $m=1,2,\cdots$ are functions of the reduced frequency. They are, in general, complex numbers. Put

$$1/\sqrt{X^{(m)}(\lambda)}=f^{(m)}(\lambda)+ig^{(m)}(\lambda) \tag{29}$$

Then the $m$th mode flutter occurs at the reduced frequency $\lambda=\lambda_F^{(m)}$ that satisfies

$$g^{(m)}\left(\lambda_F^{(m)}\right)=0 \tag{30}$$

The expressions for the $m$th mode flutter velocity and flutter frequency are, respectively, given by

$$W_{aF}^{(m)}=b_a\omega_{B1}f^{(m)}\left(\lambda_F^{(m)}\right)/\lambda_F^{(m)} \quad \text{and} \quad \omega_F^{(m)}=\omega_{B1}f^{(m)}\left(\lambda_F^{(m)}\right) \tag{31}$$

The blade motion at the $m$th mode flutter is given by

$$a^{(m)}(r,s,t)\propto e^{i\omega_F^{(m)}t}\left[\sum_{k=1}^{\infty}Z_k(r)\eta_k^{(m)}+\sum_{k=1}^{\infty}[s-s_e(r)]\Phi_k(r)\phi_k^{(m)}\right] \tag{32}$$

where

$$\begin{Bmatrix}\eta_k^{(m)}/b_a\\ \phi_k^{(m)}\end{Bmatrix}=\boldsymbol{y}_k^{(m)}\left(\lambda_F^{(m)}\right) \tag{33}$$

The most probable flutter mode will be that corresponding to the lowest flutter velocity. Hence

$$W_{aF}=b_a\omega_{B1}\min\left[f^{(1)}\left(\lambda_F^{(1)}\right)/\lambda_F^{(1)}, f^{(2)}\left(\lambda_F^{(2)}\right)/\lambda_F^{(2)},\cdots\right] \tag{34}$$

Note that to search the condition of Eq. (30) we should compute the aerodynamic force terms for various values of $\lambda$. To this end,

**Table 1 Specified conditions**

| Case | $N_{B1}$ | $\Omega_1$ | $C_{a1}$ | $N_{B2}$ | $\Omega_2$ | $C_{a2}$ |
|---|---|---|---|---|---|---|
| Sub-sub | 40 | 1.0 | 0.1 | 40 | −1.0 | 0.1 |
| Sup-sub | 30 | 3.0 | 0.0633 | 40 | −1.0 | 0.1 |

computation by CFD may be too time-consuming. On the other hand the present analytical method is a very useful aerodynamic tool, which can provide numerical values of aerodynamic force terms for a given reduced frequency within a few seconds on a modern personal computer.

## III. Numerical Results and Discussion

### A. Conditions Investigated

The results presented in this paper are restricted to cases where blades of rotor 1 (located upstream) are vibrating. In all cases the axial Mach number and the boss ratio are fixed to $M_a = 0.6$ and $h = 0.7$, respectively. Further two cases of blade row configurations shown in Table 1 are dealt with. Note that the relative flow velocity for the rotor blades is supersonic along the whole span for $\Omega_1 = 3.0$, and subsonic along the whole span for $\Omega_1 = 1.0$ or $\Omega_2 = -1.0$.

In general, it is not easy to obtain precise elastic properties of twisted blades. The main purpose of the present paper is to investigate the effect of the multiblade-row coupling on the cascade flutter. Therefore to simplify the problem, let the elastic properties be approximated by those of a uniform cantilever beam. The bending and torsional mode shape functions of the canti-lever beam are given by

$$Z_k(r) = ((\sin\Gamma_k - \sinh\Gamma_k)\{\sinh[\Gamma_k R(r)] - \sin[\Gamma_k R(r)]\} + (\cos\Gamma_k + \cosh\Gamma_k)\{\cosh[\Gamma_k R(r)] - \cos[\Gamma_k R(r)]\})/(\sin\Gamma_k \sinh\Gamma_k) \quad (35)$$

$$\Phi_k(r) = \sqrt{2}\sin\{[(2k-1)/2]\pi R(r)\} \quad (36)$$

where

$$R(r) = (r-h)/(1-h) \quad (37)$$

$$\Gamma_1 = 0.597\pi, \qquad \Gamma_2 = 1.49\pi, \qquad \Gamma_k = (2k-1)\pi/2: \ (k \geq 3) \quad (38)$$

Here the shape functions are normalized as

$$\frac{1}{1-h}\int_h^1 Z_k(r)Z_j(r)\,\mathrm{d}r = \delta_{kj}, \qquad \frac{1}{1-h}\int_h^1 \Phi_k(r)\Phi_j(r)\,\mathrm{d}r = \delta_{kj} \quad (39)$$

Further, the elastic properties of blades are assumed uniform along the span. In solving the flutter Eq. (23) vibration modes of the first and second bending orders with the natural frequencies $\omega_{B1}$ and $\omega_{B2}$ and the first and second torsion orders with the natural frequencies $\omega_{T1}$ and $\omega_{T2}$ are taken into account. The specified values are as follows: the mass ratio $\mu_{\mathrm{ba}} = 120$, the normalized distance between the center of gravity and the elastic axis $x_{\mathrm{eg}} = 0.141$, the normalized radius of gyration $r_e = \sqrt{0.6}$, and the elastic axis position $z_e/C_a = -0.075$. Further, unless otherwise stated, the natural frequency ratios are fixed to $\bar{\omega}_{T1} = \omega_{T1}/\omega_{B1} = 6.0$, $\bar{\omega}_{B2} = \omega_{B2}/\omega_{B1} = 6.3$, and $\bar{\omega}_{T2} = \omega_{T2}/\omega_{B1} = 18.0$. These values approximately correspond to the natural frequency ratios of a flat plate of aspect ratio 3.0.

### B. Case Sub-Sub

Figures 3 and 4 show the flutter reduced frequency $2\lambda_F = \omega_F C_{a1}$ and the dimensionless flutter frequency $\omega_F/\omega_{B1}$ as functions of the interblade phase parameter $\sigma$ and the distance between the blade rows $G$. Here $C_a = (C_{a1} + C_{a2})/2$, and "Isolated" implies the isolated blade row, i.e., the case of absence of rotor 2. In Fig. 3 cutoff boundaries of duct modes defined by Eq. (11) are also indicated.

In general, crucial change in the flutter frequency occurs through the cutoff boundaries of the fundamental primary duct mode (0,0;0). Further, it is clear that the effect of blade row coupling, which can be measured by the deviation from the case of the isolated blade row, is very small in the range of $\sigma$ where the fundamental primary duct mode (0,0;0) is cut off, but it is large in the range of $\sigma$ where the fundamental primary duct mode (0,0;0) is cut on. In the cases of small blade row gaps ($G = 1.1C_a$ and $G = 2.0C_a$), the blade row coupling effect is very large and enhances the flutter frequency in the cut-on region of (0,0;0) duct mode, and further it is not very small just outside the cut-on region of (0,0;0) duct mode. This indicates that the cutoff duct modes also play some role in aeroacoustic interaction between blade rows in the near field, where cutoff duct modes do not fully disappear. It is also clear that the blade row coupling effect diminishes as the blade row gap increases in the range of $\sigma$ where the fundamental primary duct mode (0,0;0) is cut off. On the other hand in the cut-on region of (0,0;0) duct mode the coupling effect never diminishes by increase of the blade row gap.

Figure 5 shows the reduced flutter velocity $W_{aF}/(b_a\omega_{B1})$. Large effect of blade row coupling is again observed in the range of $\sigma$ where (0,0;0) duct mode is cut on. It should be noted also, that in the cases of small blade row gaps ($G = 1.1C_a$ and $G = 2.0C_a$), deviation from

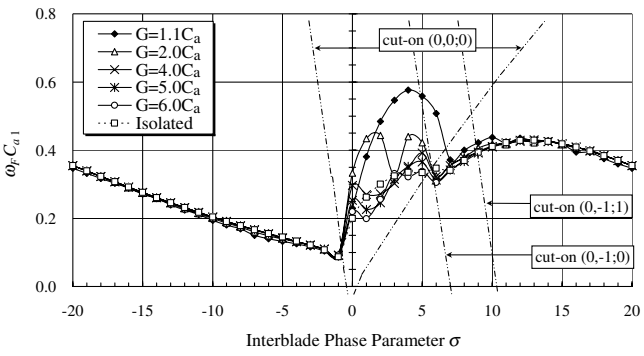


**Fig. 3 Flutter reduced frequency $\omega_F C_{a1} = 2\lambda_F$. Case sub-sub.**

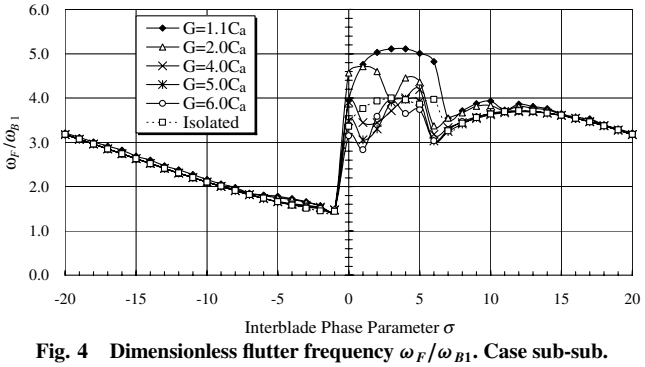


**Fig. 4 Dimensionless flutter frequency $\omega_F/\omega_{B1}$. Case sub-sub.**

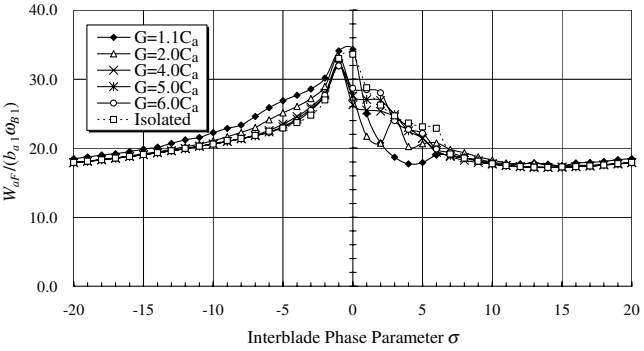


**Fig. 5 Reduced flutter velocity $W_{aF}/(b_{a1}\omega_{B1})$. Case sub-sub.**

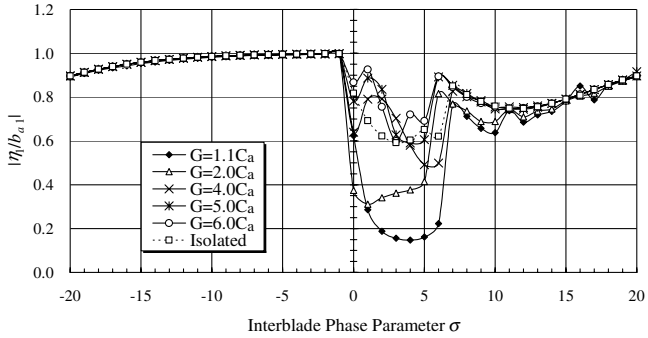


**Fig. 6 The first bending mode amplitude $|\eta_1/b_{a1}|$ at the flutter condition. Case sub-sub.**

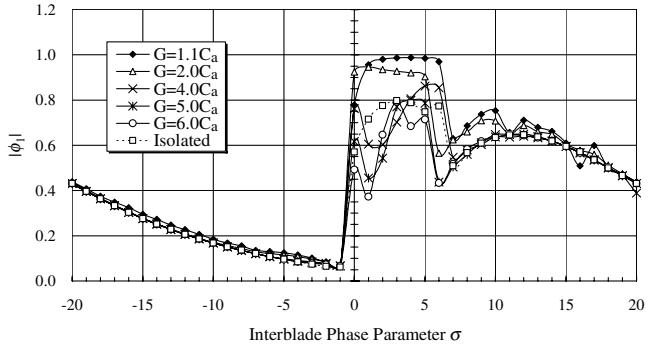


**Fig. 7 The first torsion mode amplitude $|\phi_1|$ at the flutter condition. Case sub-sub.**

the case of the isolated blade row is quite large in the cut-on region of (0,0;0) duct mode, and still significant in the cutoff region of (0,0;0) duct mode. In those cases it can be stated that the effect of blade row coupling decreases the flutter velocity in the cut-on region of the fundamental primary duct mode (0,0;0), but increases the flutter velocity outside the region.

Figures 6 and 7 show absolute values of the modal amplitudes of blade displacement at the flutter condition. First of all, drastic change in the flutter mode occurs across the cutoff boundaries of the primary duct mode (0,0;0) irrespective of the blade row coupling conditions. In the range of $\sigma$ where the fundamental primary duct mode (0,0;0) is cut off, the first bending mode $\eta_1$ is predominant at the side of negative $\sigma$, whereas the first bending mode $\eta_1$ is still larger but the dominance is smaller at the side of positive $\sigma$. On the other hand, in the range of $\sigma$ where (0,0;0) duct mode is cut on, the first torsion mode $\phi_1$ is rather dominant in the case of the isolated blade row and overwhelmingly dominant in the cases of small blade row gaps ($G = 1.1C_a$ and $G = 2.0C_a$). In the cases of longer blade row distances ($G = 4.0C_a$, $5.0C_a$, and $6.0C_a$), however, the dominance changes from the first bending mode to the first torsion mode with increase of $\sigma$.

### C. Modified Case Sub-Sub

As mentioned before, we specified the natural frequency ratios assuming a blade with an aspect ratio nearly equal to 3, and hence the first torsional frequency ratio $\omega_{T1}/\omega_{B1} = 6.0$ is rather close to the second bending frequency ratio $\omega_{B2}/\omega_{B1} = 6.3$. Then a question may arise: are we dealing with a special case of coalescence flutter? To address the question, we computed a modified case sub-sub, where are given the natural frequency ratios of $\omega_{T1}/\omega_{B1} = 4.2$, $\omega_{B2}/\omega_{B1} = 6.2$, and $\omega_{T2}/\omega_{B1} = 13.9$, which approximately correspond to the natural frequency ratios of a flat plate of aspect ratio 2.0.

Figure 8 shows the reduced flutter velocities for various blade row gaps for the modified case sub-sub. We observe no essential difference from the original case sub-sub (Fig. 5). Further, Fig. 9 shows comparison in the modal amplitudes at the flutter condition

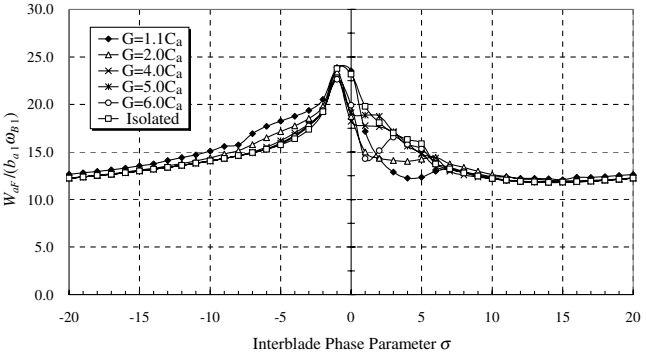


**Fig. 8 Reduced flutter velocity $W_{aF}/(b_{a1}\omega_{B1})$. The modified case sub-sub.**

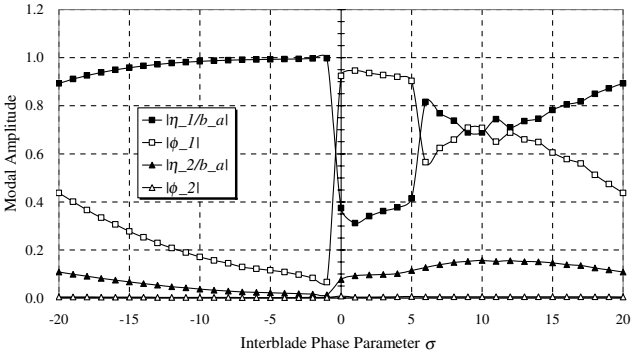


**a) Case sub-sub**

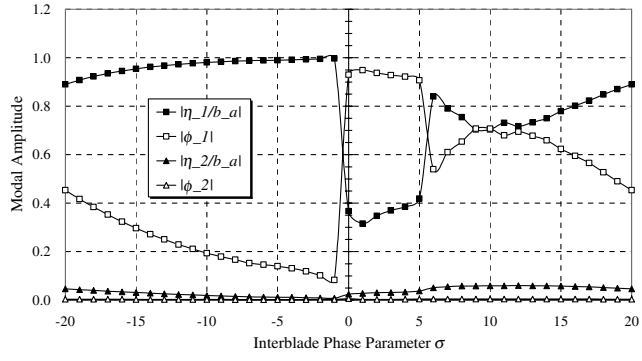


**b) The modified case sub-sub**

**Fig. 9 Modal amplitudes at the flutter condition. $G = 2.0C_a$. Comparison between the case sub-sub and the modified case sub-sub.**

between the case sub-sub (Fig. 9a) and the modified case sub-sub (Fig. 9b). Again we can see no crucial difference, although the inferiority in magnitude of the second bending mode is more conspicuous in the modified case sub-sub (Fig. 9b) of a wider natural frequency separation than in the original case sub-sub (Fig. 9a). Consequently there is no evidence that the original selection of the natural frequency ratios may cause abnormalities in the flutter condition.

### D. Case Sup-Sub

Figures 10–14 show the results of case sup-sub, where the supersonic rotor 1 of oscillating blades interacts with the subsonic rotor 2 of nonoscillating blades. First of all it should be mentioned that the flutter characteristics of the supersonic rotor is quite different from those of the subsonic rotors (case sub-sub). With respect to this matter, it should be noted that the range of $\sigma$ where the fundamental primary duct mode (0,0;0) is cut off is very narrow in the case of supersonic blade rows.

As Fig. 10 shows no flutter occurs in the range of $\sigma$ where the fundamental primary duct mode (0,0;0) is cut off. Thus in the range

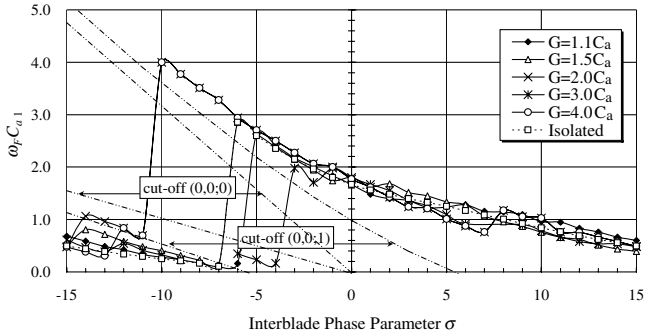


**Fig. 10 Flutter reduced frequency $\omega_F C_{a1} = 2\lambda_F$. Case sup-sub.**

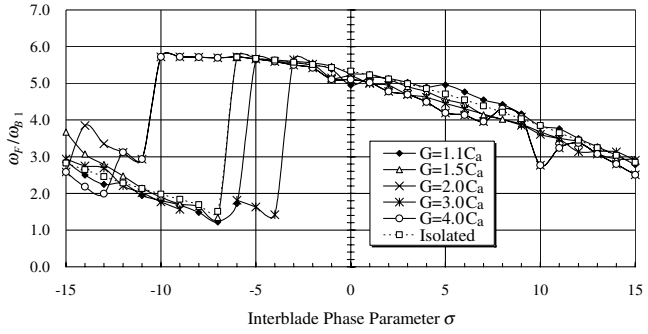


**Fig. 11 Dimensionless flutter frequency $\omega_F/\omega_{B1}$. Case sup-sub.**

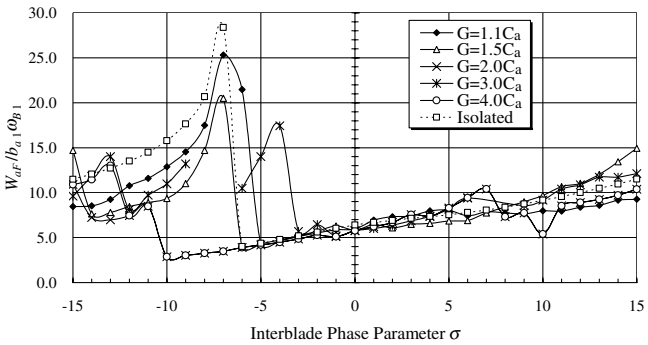


**Fig. 12 Reduced flutter velocity $W_{aF}/(b_{a1}\omega_{B1})$. Case sup-sub.**

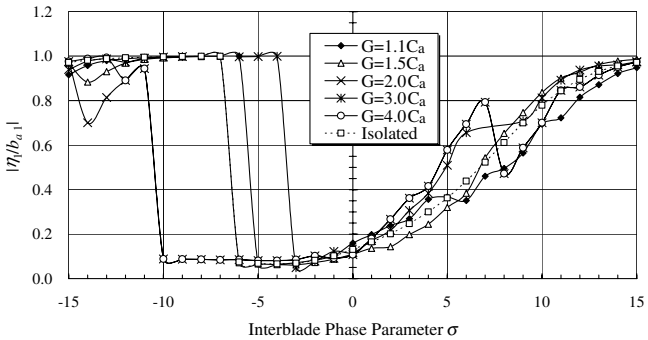


**Fig. 13 The first bending mode amplitude $|\eta_1/b_{a1}|$ at the flutter condition. Case sup-sub.**

of negative $\sigma$, the flutter reduced frequency $\omega_F C_{a1}$ and also the dimensionless flutter frequency $\omega_F/\omega_{B1}$ (Fig. 11) jump from the lower cut-on side $\omega_F < \omega^-_{(0,0;0)}$ to the upper cut-on side $\omega_F > \omega^+_{(0,0;0)}$ with a small change in $\sigma$. Note that $\sigma$ only takes integral numbers, and the jump occurs by just one step change in $\sigma$. More close observation reveals that the flutter is unlikely to occur also in the range of $\sigma$ where the second primary duct mode (0,0;1) is cut off.

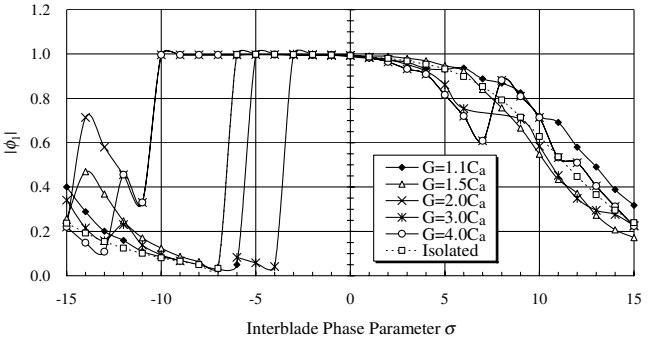


**Fig. 14 The first torsion mode amplitude $|\phi_1|$ at the flutter condition. Case sup-sub.**

A jumping up of the reduced flutter frequency is accompanied by jumping down of the reduced flutter velocity (Fig. 12), and change of dominance of the flutter mode from the first bending mode to the first torsional mode (Figs. 13 and 14).

The effect of the blade row coupling is generally large and it is worth emphasizing that the interblade phase angle across which the flutter point jumps is highly dependent on the blade row gap.

Finally it should also be pointed out that the reduced flutter velocity of the supersonic rotor (case sup-sub shown in Fig. 12) is generally lower than that of the subsonic rotor (case sub-sub shown in Fig. 5).

## IV. Conclusions

1) The effect of the neighboring blade row on the cascade flutter characteristics is closely related to the state (cut-on, cutoff, near resonance) of primary acoustic duct modes.

2) In the case of vibrating subsonic blade row the effect of blade row coupling is large in the range of the interblade phase angle where the fundamental primary duct mode is cut on.

3) In the case of vibrating subsonic blade row the closely placed neighboring blade row gives substantial influence on the reduced flutter velocity even in the range outside of the cut-on primary duct mode of the lowest order.

4) In the case of vibrating supersonic blade row no flutter occurs in the range where the fundamental primary duct mode is cut off, and the flutter point jumps across the cutoff region.

5) The interblade phase angle across which the flutter point of the supersonic blade row jumps is highly dependent on the blade row gap.

## Appendix A: Philosophy to Determine Blade Loading

The disturbance flowfield can be expressed as summation of disturbances induced by unsteady blade loadings of both rotors. In the case of vibration of rotor 1 blades expressed by Eq. (2), the disturbance velocity $\boldsymbol{q}$ is expressed in the form

$$\begin{aligned}\boldsymbol{q} = &\sum_{\nu=-\infty}^{\infty} e^{i\omega_{1\nu}t}\int_h^1\int_{-C_{a1}/2}^{C_{a1}/2}\Delta p_{1,(\nu)}(\rho,\zeta)\\ &\times \boldsymbol{K_q}(r,\xi_1,z_1-\zeta|\rho;N_{B1},\Omega_1,\omega_{1\nu},\sigma_{1\nu})\,\mathrm{d}\zeta\,\mathrm{d}\rho\\ &+\sum_{\mu=-\infty}^{\infty} e^{i\omega_{2\mu}t}\int_h^1\int_{-C_{a2}/2}^{C_{a2}/2}\Delta p_{2,(\mu)}(\rho,\zeta)\\ &\times \boldsymbol{K_q}(r,\xi_2,z_2-\zeta|\rho;N_{B2},\Omega_2,\omega_{2\mu},\sigma_{2\mu})\,\mathrm{d}\zeta\,\mathrm{d}\rho \qquad \text{(A1)}\end{aligned}$$

where $\xi_1$ and $\xi_2$ are helical coordinates defined by

$$\xi_1 = \theta_1 - \Omega_1 z_1, \qquad \xi_2 = \theta_2 - \Omega_2 z_2 \qquad \text{(A2)}$$

Note that the $m$th blade of rotor $j$ is placed on the surface $\xi_j = 2\pi m/N_{Bj}$.

The kernel function $\boldsymbol{K_q}$ denotes the disturbance velocity induced by an annular row of pressure dipoles of fluctuating strength with unit amplitude, and it is exactly same as that for a single blade row model [9,10]. It involves not only acoustic disturbances but also vortical disturbances convected downstream from the dipole points. This is further decomposed into circumferential modes in the form

$$\boldsymbol{K_q}(r,\xi,z-\zeta|\rho;N_B,\Omega,\omega,\sigma)=\sum_{\kappa=-\infty}^{\infty}e^{i(\kappa N_B+\sigma)\xi}\times\boldsymbol{K_q^{(\kappa)}}(r,z-\zeta|\rho;N_B,\Omega,\omega,\sigma) \tag{A3}$$

We should note that the blade loadings are not prescribed but should be determined so that the disturbance velocity given by Eq. (A1) satisfies the flow tangency condition on the blade surfaces of both rotors. Here it is worth emphasizing that the expression (A1) with the blade loading functions determined in this way automatically includes phenomena of reflection and transmission of disturbances at the rotors.

The flow tangency condition at the blade surfaces can be expressed by

$$[q_{\perp 1}]_{\xi_1=0}=(i\omega a(r,z_1)+\partial a(r,z_1)/\partial z_1)e^{i\omega t}:\ -C_{a1}/2\le z_1\le C_{a1}/2 \tag{A4}$$

$$[q_{\perp 2}]_{\xi_2=0}=0:\ C_{a2}/2\le z_2\le C_{a2}/2 \tag{A5}$$

Equations (A4) and (A5) can be rewritten into a set of simultaneous integral equations for the unsteady blade loading functions as follows:

$$\int_h^1\int_{-C_{a1}/2}^{C_{a1}/2}\Delta p_{1,(\nu)}(\rho,\zeta)K_{q\perp 1}(r,0,z_1-\zeta|\rho;N_{B1},\Omega_1,\omega_{1\nu},\sigma_{1\nu})\,\mathrm{d}\zeta\,\mathrm{d}\rho+\sum_{\mu=-\infty}^{\infty}e^{i(\mu N_{B1}+\sigma_{1\nu})\{(\Omega_1-\Omega_2)z_1+\Omega_2 G\}}\int_h^1\int_{-C_{a2}/2}^{C_{a2}/2}\Delta p_{2,(\mu)}(\rho,\zeta)\times K_{q\perp 1}^{(\nu)}(r,0,z_1-G-\zeta|\rho;N_{B2},\Omega_2,\omega_{2\mu},\sigma_{2\mu})\,\mathrm{d}\zeta\,\mathrm{d}\rho=\{i\omega a(r,z_1)+\partial a(r,z_1)/\partial z_1\}\delta_{\nu 0}:\ -C_{a1}/2\le z_1\le C_{a1}/2 \tag{A6}$$

$$\int_h^1\int_{-C_{a2}/2}^{C_{a2}/2}\Delta p_{2,(\nu)}(\rho,\zeta)K_{q\perp 2}(r,0,z_2-\zeta|\rho;N_{B2},\Omega_2,\omega_{2\nu},\sigma_{2\nu})\,\mathrm{d}\zeta\,\mathrm{d}\rho+\sum_{\mu=-\infty}^{\infty}e^{-i(\mu N_{B2}+\sigma_{2\nu})\{(\Omega_1-\Omega_2)z_2+\Omega_1 G\}}\int_h^1\int_{-C_{a1}/2}^{C_{a1}/2}\Delta p_{1,(\mu)}(\rho,\zeta)\times K_{q\perp 2}^{(\nu)}(r,0,z_2+G-\zeta|\rho;N_{B1},\Omega_1,\omega_{1\mu},\sigma_{1\mu})\,\mathrm{d}\zeta\,\mathrm{d}\rho=0:\ -C_{a2}/2\le z_2\le C_{a2}/2,\ \text{for } \nu=0,\pm1,\pm2,\ldots \tag{A7}$$

Truncating the infinite series into finite series, one can numerically solve the equations by a standard method.

The mathematical process to derive the kernel functions and their expressions are omitted to save space, but can be referred to [9,10].

In the case of blade vibration of rotor 2, similar formulations can be made.

## Appendix B: Definitions of Parameters in Matrices $M_{kj}$, $S_{kj}$, $K_{kj}$, and $A_{kj}$

Mass per unit span of a blade $m(r)$, moment of inertia per unit span of a blade $I_e(r)$, and static mass moment per unit span of a blade $S_e(r)$are defined as follows:

$$m(r)=r_T^*\int_{-b(r)}^{b(r)}\rho_b(r,s)\,\mathrm{d}s \tag{B1}$$

$$I_e(r)=r_T^{*3}\int_{-b(r)}^{b(r)}\rho_b(r,s)\{s-s_e(r)\}^2\,\mathrm{d}s \tag{B2}$$

$$S_e(r)=r_T^{*2}\int_{-b(r)}^{b(r)}\rho_b(r,s)\{s-s_e(r)\}\,\mathrm{d}s \tag{B3}$$

Here $\rho_b(r,s)$ denotes the blade mass per unit blade surface area.

Note that each set of the natural mode shape functions $Z_1(r),Z_2(r),\cdots$ and $\Phi_1(r),\Phi_2(r),\cdots$ is orthogonal with weight functions $m(r)$ and $I_e(r)$ as follows:

$$r_T^*\int_h^1 m(r)Z_k(r)Z_j(r)\,\mathrm{d}r=M_j\delta_{kj} \tag{B4}$$

$$r_T^*\int_h^1 I_e(r)\Phi_k(r)\Phi_j(r)\,\mathrm{d}r=I_j\delta_{kj} \tag{B5}$$

Equations (B4) and (B5) also define generalized mass $M_j$ and generalized moment of inertia $I_j$, respectively. We further define modal static mass moment $S_{kj}$ by

$$S_{kj}=r_T^*\int_h^1 S_e(r)Z_j(r)\Phi_k(r)\,\mathrm{d}r \tag{B6}$$

The modal lift and moment coefficients are defined by

$$\begin{Bmatrix}L_{Bkj}\\L_{Tkj}\end{Bmatrix}=\frac{1}{\pi(1-h)}\int_h^1 Z_k(r)\,\mathrm{d}r\frac{1}{b_a}\int_{-b(r)}^{b(r)}\begin{Bmatrix}\Delta p_{Bj}(r,s)\\\Delta p_{Tj}(r,s)\end{Bmatrix}\mathrm{d}s \tag{B7}$$

$$\begin{Bmatrix}M_{Bkj}\\M_{Tkj}\end{Bmatrix}=\frac{1}{\pi(1-h)}\int_h^1 \Phi_k(r)\,\mathrm{d}r\frac{1}{b_a^2}\int_{-b(r)}^{b(r)}\begin{Bmatrix}\Delta p_{Bj}(r,s)\\\Delta p_{Tj}(r,s)\end{Bmatrix}\times\{s-s_e(r)\}\,\mathrm{d}s \tag{B8}$$

We can define total mass of a blade $M_b$, total moment of inertia of a blade $I_{\mathrm{be}}$, and total static mass moment of a blade $S_{\mathrm{be}}$ by

$$M_b=r_T^*\int_h^1 m(r)\,\mathrm{d}r \tag{B9}$$

$$I_{\mathrm{be}}=r_T^*\int_h^1 I_e(r)\,\mathrm{d}r \tag{B10}$$

$$S_{\mathrm{be}}=r_T^*\int_h^1 S_e(r)\,\mathrm{d}r \tag{B11}$$

Further, we denote mass of air in a cylindrical volume of radius $r_T^*b_a$ and height $r_T^*(1-h)$ by

$$M_{\mathrm{air}}=r_T^{*3}\pi b_a^2(1-h)\rho_0^* \tag{B12}$$

Then we obtain mass ratio, average dimensionless distance between the center of gravity and the elastic axis, and average dimensionless radius of gyration as follows:

$$\mu_{\mathrm{ba}}=M_b/M_{\mathrm{air}},\qquad x_{\mathrm{eg}}=S_{\mathrm{be}}/\left(M_b r_T^* b_a\right),\qquad r_e=\sqrt{I_{\mathrm{be}}/\left(M_b r_T^{*2} b_a^2\right)} \tag{B13}$$

Finally dimensionless generalized modal mass, modal moment of inertia, and modal static mass moment are defined by

$$\bar{M}_k=M_k/M_b,\qquad \bar{I}_k=I_k/I_{\mathrm{be}},\qquad \bar{S}_{kj}=S_{kj}/S_{\mathrm{be}} \tag{B14}$$

## Acknowledgment

This work was funded by Grants-in-Aid for Scientific Research of Japan Society for the Promotion of Science.

## References

[1] Tanida, Y., "Effect of Blade Row Interference on Cascade Flutter," *Transactions of the Japan Society for Aeronautical and Space Sciences*, Vol. 9, No. 15, 1966, pp. 100–108.

[2] Kobayashi, H., Tanaka, H., and Maruta, H., "Effect of Interference Between Moving Blade Rows on Cascade Flutter, 1st Report: Experiment on Compressor Cascade in Flexure Mode" (in Japanese), *Transactions of the Japan Society for Mechanical Engineers*, Vol. 40, No. 334, 1974, pp. 1615–1626.

[3] Kobayashi, H., Tanaka, H., and Hanamura, Y., "Effect of Interference Between Moving Blade Rows on Cascade Flutter, 2nd Report: Theoretical Analysis of Flexure Mode" (in Japanese), *Transactions of the Japan Society for Mechanical Engineers*, Vol. 41, No. 346, 1975, pp. 1770–1780.

[4] Butenko, K. K., and Osipov, A. A., "Unsteady Subsonic Flow Past Two Relatively Moving Flat Cascades of Thin Weakly Loaded Oscillating Blades," *Fluid Dynamics*, Vol. 22, Plenum Publishing Corporation, New York, 1989, pp. 620–625.

[5] Hall, K. C., and Silkowski, P. D., "The Influence of Neighboring Blade Rows on the Unsteady Aerodynamic Response of Cascades," *Journal of Turbomachinery*, Vol. 119, No. 1, Jan. 1997, pp. 85, 93.

[6] Namba, M., Yamasaki, N., and Nishimura, S., "Unsteady Aerodynamic Force on Oscillating Blades of Contra-Rotating Annular Cascades," *Unsteady Aerodynamics, Aeroacoustics and Aeroelasticity of Turbomachines*, edited by P. Ferrand and S. Aubert, Presses Universitaires de Grenoble, Grenoble, France, 2001, pp. 375–386.

[7] Namba, M., and Nanba, K., "Unsteady Aerodynamic Work on Oscillating Annular Cascades in Counter Rotation: Combination of Supersonic and Subsonic Cascades," *Unsteady Aerodynamics, Aeroacoustics and Aeroelasticity of Turbomachines*, edited by K. C. Hall, R. E. Kielb, and J. P. Thomas, Springer, New York, 2006, pp. 177–188.

[8] Hall, K. C., Ekici, K., and Voytovych, D. M., "Multistage Coupling for Unsteady Flows in Turbomachinery," *Unsteady Aerodynamics, Aeroacoustics and Aeroelasticity of Turbomachines*, edited by K. C. Hall, R. E. Kielb, and J. P. Thomas, Springer, New York, 2006, pp. 217–229.

[9] Namba, M., and Ishikawa, A., "Three-Dimensional Aerodynamic Characteristics of Oscillating Supersonic and Transonic Annular Cascades," *Journal of Engineering for Power*, Vol. 105, No. 1, Jan. 1983, pp. 138–146.

[10] Namba, M., "Three-Dimensional Flows," *AGARD Manual on Aeroelasticity in Axial Flow Turbomachines*, Vol. 1, Unsteady Turbomachinery Aerodynamics, AGARD-AG-298, edited by M. F. Platzer and F. O. Carta, Neuilly sur Seine, France, 1987.

E. Livne
*Associate Editor*